DOI: 10.1002/ejic.200600721

Synthesis, Structure and Surface Photovoltage of a Series of Ni^{II} Coordination Polymers

Li-Ping Sun,[a] Shu-Yun Niu,*[a] Jing Jin,[a] Guang-Di Yang,[b] and Ling Ye[b]

Keywords: Coordination polymers / Nickel / Hydrogen bonds / Surface photovoltage spectroscopy

Three novel Ni^{II} coordination polymers $[Ni_2(HCOO)_4(H_2O)_4]_n$ (**1**), $[Na_2Ni(btec)(H_2O)_8]_n$ (**2**; H_4btec = 1,2,4,5-benzenetetracarboxylic acid) and $[\{Ni(pdc)(H_2O)_2\}\cdot H_2O]_n$ (**3**; H_2pdc = pyridine-2,5-dicarboxylic acid) have been hydrothermally synthesized and their structures determined by single-crystal X-ray diffraction. The formate groups in complex **1** bridge the Ni^{II} ions to form a infinite 3D structure. Complex **2** also possesses a infinite 3D structure and the coordination environment of the Ni^{II} ion is a perfect octahedron. Complex **3** is a 2D infinite coordination polymer. The surface photovoltage spectra of complexes **1**–**3** indicate that they all show three positive surface photovoltage (SPV) responses in the range of 300–800 nm and all show p-type semiconductor characteristics. Although the intensities of the SPV responses are obviously different, this can mainly be attributed to the difference of their structures. The field-induced surface photovoltage spectra (FISPS) of complexes **1**–**3** confirm their p-type semiconductor characteristics.

Introduction

Metal–organic coordination polymers are receiving ever increasing attention owing to their potential applications in functional materials for use in fields such as magnetism, catalysis, electrical conductivity, optical materials, host–guest chemistry, and biomimetic chemistry.[1–5] The design and synthesis of the coordination polymers have therefore undergone rapid development in the areas of coordination and supramolecular chemistry.[6–9] Carboxylate groups often play an important role in the construction of polynuclear complexes as they can adapt many types of bridging pattern, e.g. *syn-syn*, *anti-anti*, *syn-anti* and mono-monodentate and mono-didentate etc.,[10–12] which result in a variety of structural frameworks. They can also act as both donors and acceptors of hydrogen bonds depending on whether the carboxylic O atoms are deprotonated or not.[13] The existence of a variety of hydrogen bonds therefore enriches the function of a coordination supramolecule.

The energy gaps of some transition metal coordination polymers with unique structures are sometimes in the region of those of semiconductors, which means that they can show semiconductor characteristics and can therefore be regarded as a kind of inorganic–organic hybrid semiconductor. The detection of the surface charge behavior and photoelectric properties of the coordination polymers would therefore allow further research on the function of these coordination polymers. To date, reports on this aspect have focused mainly on coordination complexes with phthalocyanines or porphyrins as ligands;[14–17] there are few reports on the coordination polymers.[18] Surface photovoltage spectroscopy (SPS) is a highly sensitive tool that can be used to investigate the photophysics of photogenerated species or excited states without any sample contamination or destruction.[19,20] This technique has been used to investigate photoelectric processes such as charge transfer and photocatalysis.[21] On the basis of the principle of SPS, Wang et al. have developed a field-induced surface photovoltage spectroscopy (FISPS) technique,[22,23] which they have used to investigate the photoelectric properties of semiconductors under the effect of an external electric field. We have also attempted to detect the surface charge behavior of coordination polymers with semiconductor characteristics using these techniques. In this paper we report the synthesis, structure, and surface photovoltage properties of three Ni^{II} coordination polymers. The three complexes all contain carboxylic groups as the basic building unit. Their similarities and differences in the structures are beneficial when it comes to exploring the relationship between the structural and photoelectric properties.

[a] School of Chemistry and Chemical Engineering, Liaoning Normal University,
Dalian 116029, P. R. China
E-mail: syniu@sohu.com
[b] Key Lab of Supramolecular Structure and Materials of Ministry of Education, Jilin University,
Changchun 130023, P. R. China
Supporting information for this article is available on the WWW under http://www.eurjic.org or from the author.

Result and Discussion

Synthesis and General Discussion

The synthesis of complex **1** is intriguing. The ligand in complex **1** is a formate, which was not added as one of the

starting materials. The starting materials *o*-phthalic acid and 2,2′-bipyridyl do not take part in the coordination. The synthetic procedure involves dmf and H_2O as solvents, and we think the formate group comes from dmf. This phenomenon has been reported previously,[24] and it has long been known that dmf can be hydrolyzed to formate and dma and that the rate of this process increases under basic conditions. We repeated the synthesis of complex **1** in the absence of dmf and obtained the complex [Ni(*o*-phthalate)(2,2′-bipyridyl)(H_2O)]·H_2O, which further confirms the involvement of dmf in the synthesis of complex **1**.

The synthesis of complex **2** is also interesting. The original purpose of adding NaOH was to deprotonate and to adjust the pH. However, the Na^+ ions not only balance the charge but also participate in coordination.

Structure Descriptions

The crystal data and structure refinement of complexes **1**–**3** are summarized in the Experimental Section; selected bond lengths and angles are listed in Table 1.

$[Ni_2(HCOO)_4(H_2O)_4]_n$ (1)

The single-crystal X-ray diffraction analysis revealed that complex **1** exhibits a infinite 3D framework structure whose building unit is $[Ni_2(HCOO)_4(H_2O)_4]$ (Figure 1). There are two kinds of crystallographically independent Ni^{II} ions. Ni1 is coordinated by six O atoms from six different formate O atoms, with O1, O1d, O3, and O3d atoms comprising the equatorial plane. The Ni1–O1 and Ni1–O3 bond lengths are 2.058(2) and 2.104(2) Å, respectively. The O1–Ni1–O1d and O3–Ni1–O3d bond angles are both 180°, and the O1–Ni1–O3 and O1d–Ni1–O3 bond angles are 92.98(8)° and 87.02(8)°, respectively. O2 and O2e occupy the apical positions. The Ni1–O2 bond length of 2.039(2) Å and the O2–Ni1–O2e bond angle of 180° mean that the coordination environment of Ni1 is a perfect octahedron. The other crystallographically independent Ni2 ion is also six coordinate, with two O atoms from two bridging formate O atoms and the other four O atoms from four coordinated water molecules. The formate groups in the crystal adopt an *anti-anti* coordination mode that links the Ni1 ions into a 1D infinite chain. The Ni1 ions of adjacent chains are further con-

Table 1. Selected bond lengths [Å] and angles [°] for complexes **1**–**3**.[a]

1					
Ni(1)–O(2)^{i}	2.039(2)	Ni(1)–O(3)	2.104(2)	Ni(2)–O(6)^{ii}	2.067(2)
Ni(1)–O(2)	2.039(2)	Ni(1)–O(3)^{i}	2.104(2)	Ni(2)–O(6)	2.067(2)
Ni(1)–O(1)	2.058(2)	Ni(2)–O(5)	2.026(2)	Ni(2)–O(4)	2.099(2)
Ni(1)–O(1)^{i}	2.058(2)	Ni(2)–O(5)^{ii}	2.026(2)	Ni(2)–O(4)^{ii}	2.099(2)
O(2)^{i}–Ni(1)–O(2)	180.00(8)	O(2)^{i}–Ni(1)–O(3)^{i}	87.28(8)	O(6)^{ii}–Ni(2)–O(6)	180.0
O(2)^{i}–Ni(1)–O(1)	90.52(8)	O(2)–Ni(1)–O(3)^{i}	92.72(8)	O(5)–Ni(2)–O(4)	89.57(11)
O(2)–Ni(1)–O(1)	89.48(8)	O(1)–Ni(1)–O(3)^{i}	87.02(8)	O(5)^{ii}–Ni(2)–O(4)	90.43(11)
O(2)^{i}–Ni(1)–O(1)^{i}	89.48(8)	O(1)^{i}–Ni(1)–O(3)^{i}	92.98(8)	O(6)^{ii}–Ni(2)–O(4)	90.71(7)
O(2)–Ni(1)–O(1)^{i}	90.52(8)	O(3)–Ni(1)–O(3)^{i}	180.0	O(6)–Ni(2)–O(4)	89.29(7)
O(1)–Ni(1)–O(1)^{i}	180.00(5)	O(5)–Ni(2)–O(5)^{ii}	180.0	O(5)–Ni(2)–O(4)^{ii}	90.43(11)
O(2)^{i}–Ni(1)–O(3)	92.72(8)	O(5)–Ni(2)–O(6)^{ii}	89.34(9)	O(5)^{ii}–Ni(2)–O(4)^{ii}	89.57(11)
O(2)–Ni(1)–O(3)	87.28(8)	O(5)^{ii}–Ni(2)–O(6)^{ii}	90.66(9)	O(6)^{ii}–Ni(2)–O(4)^{ii}	89.29(7)
O(1)–Ni(1)–O(3)	92.98(8)	O(5)–Ni(2)–O(6)	90.66(9)	O(6)–Ni(2)–O(4)^{ii}	90.71(7)
O(1)^{i}–Ni(1)–O(3)	87.02(8)	O(5)^{ii}–Ni(2)–O(6)	89.34(9)	O(4)–Ni(2)–O(4)^{ii}	180.0
2					
Ni(1)–O(2)	2.075(2)	Ni(1)–O(1)^{iii}	2.0767(15)	Ni(1)–O(1)^{v}	2.0767(15)
Ni(1)–O(2)^{iii}	2.075(2)	Ni(1)–O(1)	2.0767(15)	Ni(1)–O(1)^{iv}	2.0767(15)
Na(1)–O(3)	2.332(2)	Na(1)–O(3)^{vi}	2.332(2)	Na(1)–O(4)^{vi}	2.402(2)
Na(1)–O(5)^{vi}	2.5705(19)				
O(2)–Ni(1)–O(2)^{iii}	180.0	O(1)^{iii}–Ni(1)–O(1)	180.0	O(2)–Ni(1)–O(1)^{v}	85.95(5)
O(2)–Ni(1)–O(1)^{iii}	94.05(5)	O(2)–Ni(1)–O(1)^{iv}	94.05(5)	O(2)^{iii}–Ni(1)–O(1)^{v}	94.05(5)
O(2)^{iii}–Ni(1)–O(1)^{iii}	85.95(5)	O(2)^{iii}–Ni(1)–O(1)^{iv}	85.95(5)	O(1)^{iii}–Ni(1)–O(1)^{v}	86.86(9)
O(2)–Ni(1)–O(1)	85.95(5)	O(1)^{iii}–Ni(1)–O(1)^{iv}	93.14(9)	O(1)–Ni(1)–O(1)^{v}	93.14(9)
O(2)^{iii}–Ni(1)–O(1)	94.05(5)	O(1)–Ni(1)–O(1)^{iv}	86.86(9)	O(1)^{iv}–Ni(1)–O(1)^{v}	180.0
O(3)–Na(1)–O(3)^{vi}	180.00(9)	O(3)^{vi}–Na(1)–O(4)^{vi}	83.10(8)	O(3)^{vi}–Na(1)–O(5)^{vi}	79.06(9)
O(3)–Na(1)–O(4)^{vi}	96.90(8)	O(3)–Na(1)–O(5)^{vi}	100.94(9)	O(4)^{vi}–Na(1)–O(5)^{vi}	92.17(9)
3					
Ni(1)–O(1)	2.0340(15)	Ni(1)–O(3)	2.0350(15)	Ni(1)–O(2)	2.1064(15)
Ni(1)–O(7)	2.0344(16)	Ni(1)–N(1)	2.0843(17)	Ni(1)–O(4)	2.1110(14)
O(1)–Ni(1)–O(7)	97.48(7)	O(3)–Ni(1)–N(1)	79.63(6)	O(1)–Ni(1)–O(4)	86.71(6)
O(1)–Ni(1)–O(3)	173.04(6)	O(1)–Ni(1)–O(2)	86.74(7)	O(7)–Ni(1)–O(4)	92.28(6)
O(7)–Ni(1)–O(3)	88.08(7)	O(7)–Ni(1)–O(2)	89.46(6)	O(3)–Ni(1)–O(4)	97.28(6)
O(1)–Ni(1)–N(1)	94.47(7)	O(3)–Ni(1)–O(2)	89.14(6)	N(1)–Ni(1)–O(4)	93.74(6)
O(7)–Ni(1)–N(1)	166.90(6)	N(1)–Ni(1)–O(2)	85.88(7)	O(2)–Ni(1)–O(4)	173.39(6)

[a] Symmetry transformations used to generate equivalent atoms: i: $-x + 1, -y, -z + 1$; ii: $-x + 2, -y + 1, -z + 1$; iii: $-x, -y, -z - 2$; iv: $-x, y, -z - 2$; v: $x, -y, z$; vi: $-x + 1/2, -y + 1/2, -z - 1$.

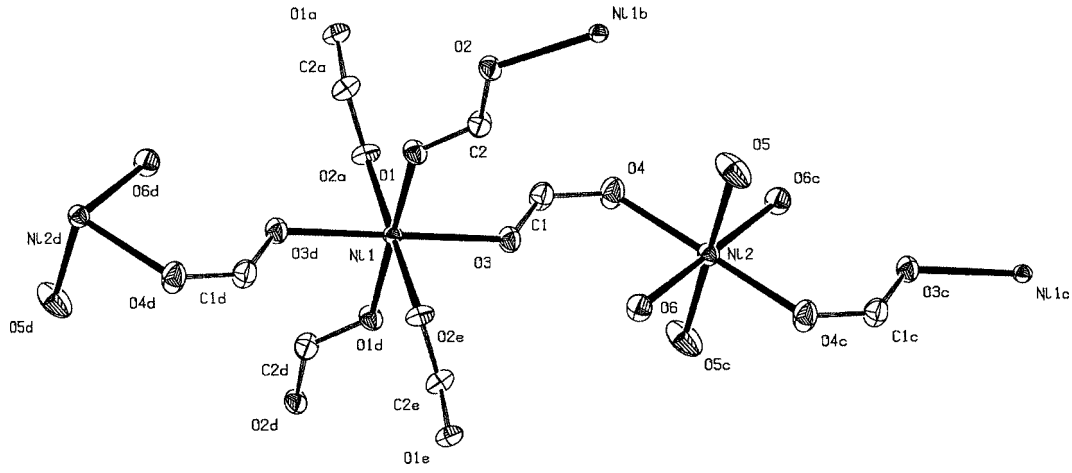

Figure 1. The ORTEP structure of complex **1** (30% probability thermal ellipsoids) showing the asymmetric unit.

nected to another 1D infinite chain along the perpendicular direction with the same mode, which means that the Ni1 ions are linked into a 2D layer in the *bc* plane (Figure 2). The coplanarity of this 2D layer is very good, and the Ni2 ions array regularly between the 2D layers. The formate groups, which lie between the Ni1 and Ni2 ions, connect these ions in a *syn-anti* mode to form a 1D infinite chain. This 1D infinite chain is perpendicular to the 2D layer, and the 2D layers are further connected into a infinite 3D structure (Figure 3). When projected along the *a* axis, it can clearly be seen that every four Ni1 ions form a rhombic hole. The sides of each rhombus are 5.808 Å and they extend infinitely along the *a* axis. The Ni2 ions lie between the holes (Figure 4).

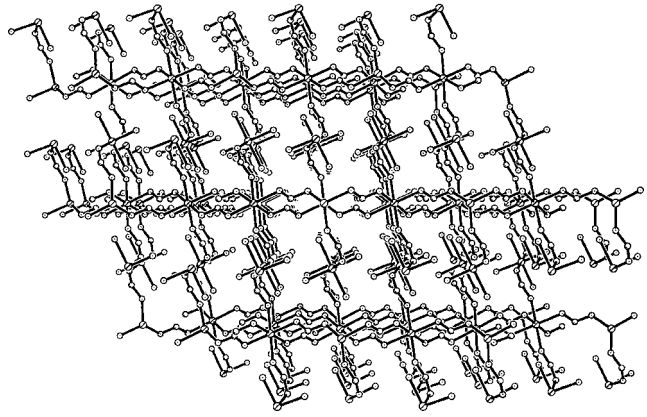

Figure 3. The 3D structure of complex **1**.

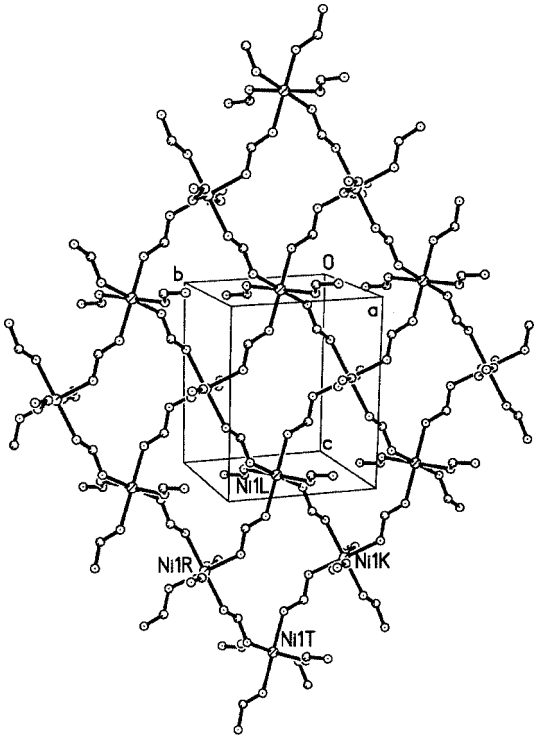

Figure 2. The 2D layer structure of Ni1 ions in complex **1**.

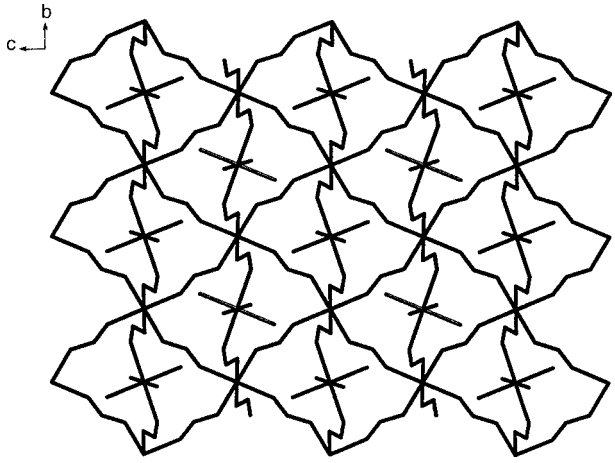

Figure 4. A projection of complex **1** along the *a* axis showing the Ni2 ions lying between the Ni1 holes.

$[Na_2Ni(btec)(H_2O)_8]_n$ (2)

Complex **2** possesses a infinite 3D structure and its building unit is $[Na_2Ni(btec)(H_2O)_8]$ (Figure 5). Each Ni^{II} ion is coordinated by six O atoms and its coordination environment is a perfect octahedron. Four O atoms (O1, O1A, O1B, O1C) are from four different btec groups, and these

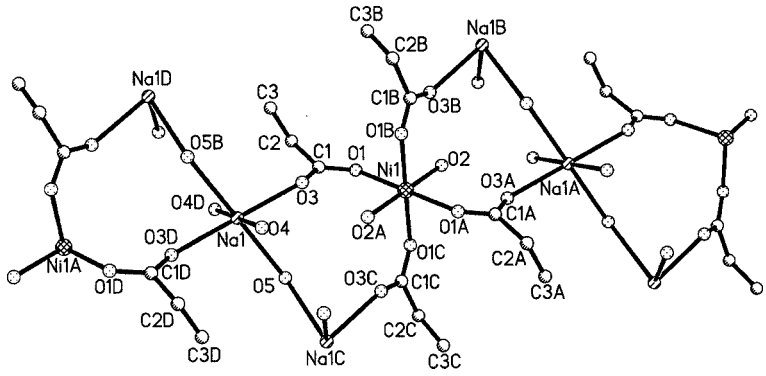

Figure 5. The building unit of complex **2**.

comprise the equatorial plane. The Ni–O1 bond length is 2.0767(15) Å and the O1A–Ni1–O1 and O1B–Ni1–O1C bond angles are all 180°. The O1–Ni1–O1B and O1–Ni1–O1C bond angles are 86.86(9)° and 93.14(9)°, respectively. The other two O atoms (O2, O2A) are from two coordinated water molecules and they occupy the apical positions of the octahedron. The Ni–O2 bond length is 2.075(2) Å and the O2–Ni–O2A bond angle is 180°.

The Na^{I} ion is coordinated by six O atoms. Two O atoms are from two btec groups and four O atoms from four coordinated water molecules, all of which comprise the distorted octahedral coordination environment of Na^{I}. In the crystal, each btec group coordinates to four different Ni^{II} ions through the four deprotonated carboxylic O atoms in a monodentate manner. Thus, the Ni^{II} ions are connected to two perpendicular 1D chains in the *bc* plane. The coplanarity of the *bc* layer is very good. The *o*- and *m*-carboxylate moieties of each btec group separately link the different Ni^{II} ions and form two kinds of multi-membered rings. The Ni1G–Ni1H (along the *c* axis) and Ni1H–Ni1B (along the *b* axis) distances are 6.086 and 9.488 Å, respectively (Figure 6). The Na^{I} ions array along the *bc* plane and link two Ni^{II} ions in the adjacent layer through the carboxylate group, which means that the 2D layers are further connected to form an infinite 3D structure (Figure 7). In addition, there are a lot of hydrogen bonds in the crystal. There are interactions between the coordinated water molecules and coordinated water molecules [O2–H···O5 2.808(3), O4–H···O4 3.145(6) Å] as well as coordinated carboxylate O atoms [O4–H···O3 3.098(3), O2–H···O3 2.608(2), O4–H···O1 3.098(3) Å]. These hydrogen bonds increase the stability of the structure.

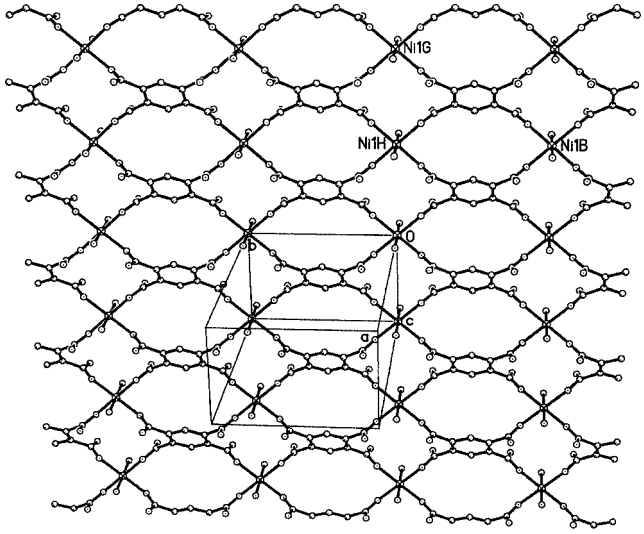

Figure 6. The 2D infinite layered structure of Ni^{II} ions in complex **2**.

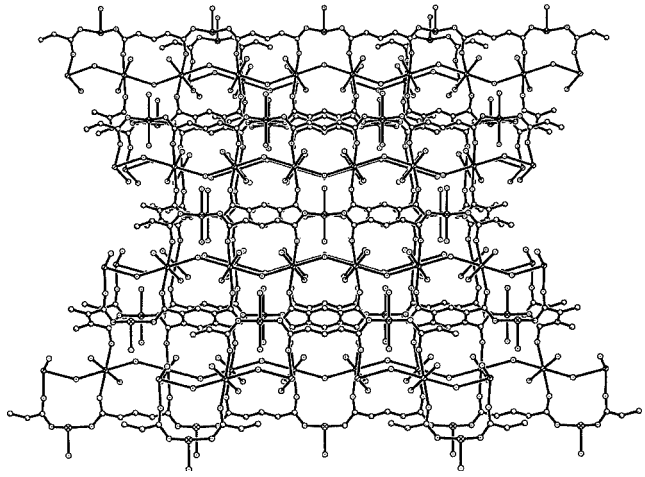

Figure 7. The 3D structure of complex **2**.

$[\{Ni(pdc)(H_2O)_2\}\cdot H_2O]_n$ (3)

The structure of complex **3** has been reported previously by Min, Dongwon et al.,[25] therefore here we place more emphasis on its SPS and FISPS properties. Complex **3** is a 2D infinite coordination polymer and its asymmetric unit is $[\{Ni(pdc)(H_2O)_2\}\cdot H_2O]$. Each Ni^{II} ion is coordinated by five O atoms and one N atom. One O atom and one N atom are from the same pdc group; the other four O atoms are from two different pdc groups and two coordinated water molecules (Figure 8). The coordination geometry around the Ni^{II} ion is a distorted octahedron. The equatorial plane is defined by O2, O7, O4, and N1 and the apical position is occupied by O3 and O1. The O3–Ni–O1 bond

angle is 173.04(6)°. In the crystal, the pdc group plays a bridging role: the α-carboxylate O atom together with the pyridine N atom coordinate to one Ni^{II} ion and the other carboxylate O atom coordinates to another Ni^{II} ion in a monodentate mode. The Ni^{II} ions are linked into a 1D infinite chain along the *a* axis. Each β-carboxylate O atom of the pdc group binds to one Ni^{II} ion in a monodentate mode to form a zigzag chain along the *b* axis, so complex **3** is further connected into a 2D waved structure (Figure 9). There are five kinds of O–H···O hydrogen bonds in the crystal. These are the interactions between the coordinated water molecules and coordinated carboxylic O atoms [O7–H···O4 2.687(12), O1–H···O3 2.696(2) Å] as well as the uncoordinated carboxylic O atom [O1–H···O5 2.726(2) Å]. The other three types of hydrogen bond are between the lattice water molecule and the coordinated water molecule [O7–H···O6 2.625(3) Å], the coordinated carboxylic O atom [O6–H···O2 2.904(3) Å], and the uncoordinated carboxylic O atom [O6–H···O5 3.051(3) Å]. Complex **3** is further connected into a 3D web by hydrogen bonds (Figure 10).

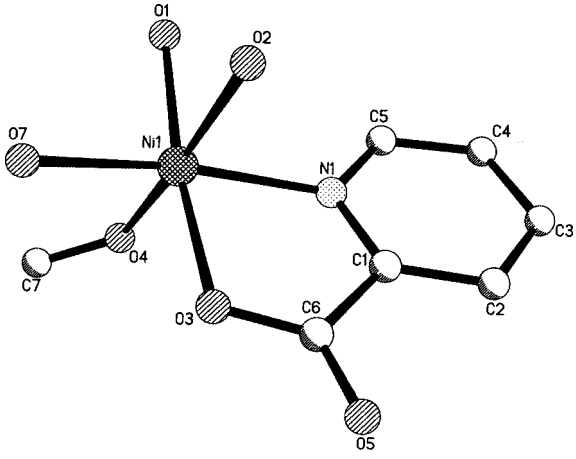

Figure 8. The asymmetric unit of complex **3**.

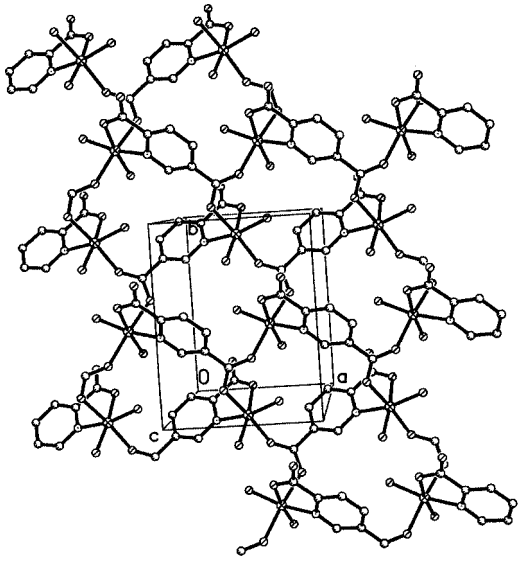

Figure 9. The 2D infinite structure of complex **3**.

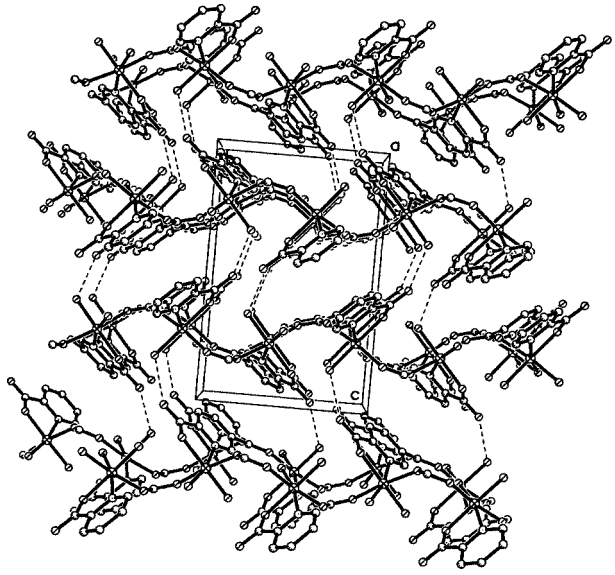

Figure 10. The 3D structure of complex **3**. Dotted lines indicate hydrogen bonds.

Surface Photovoltage Spectra of Complexes

Surface photovoltage spectra were measured with a solid junction photovoltaic cell (ITO/sample/ITO) in the range 300–800 nm. A signal detected by SPS is equivalent to the change in the surface potential barrier on illumination (δV_s), which is given by the equation

$$\delta V_s = V_s' - V_s°$$

where $V_s°$ and V_s' are the surface potential barriers before and after illumination, respectively. As far as band-to-band transitions are concerned, a positive response of SPV ($\delta V_s > 0$) means that the sample is characterized as a p-type semiconductor, whereas a negative response means that the sample is an n-type semiconductor. The magnitude of the surface potential barrier depends on the number of surface net charges. Figures 11 and 12 show the SPS spectra of complexes **1** and **3**, respectively. The SPS spectrum of complex **2** is similar to that of complex **1**. The SPV responses at 300–500 nm show some overlap, but they can be separated by treating them with the program Origin 7.0[26]. Complexes **1**–**3** all show three positive SPV responses in the range 300–800 nm, which indicates that they all have p-type semiconductor characteristics. The response bands at λ_{max} = 342 nm can be attributed to an LMCT (ligand to metal charge transfer) transition. In contrast with a previous report,[18] the LMCT bands are blue-shifted. The complexes reported here are mainly coordinated by O atoms, in contrast to the other complexes, which are mainly coordinated by N atoms,[18] therefore, as the electronegativity of oxygen is larger than that of nitrogen, more energy is needed to produce the LMCT, which means that the LMCT band is blue-shifted. The responses at λ_{max} = 392 (**1**), 387 (**2**), and 396 nm (**3**) can be assigned to the d→d* transition of Ni^{II} [$^3A_{2g}\rightarrow{}^3T_{1g}$ (^3P)], and the response bands between 600 and

800 nm can be attributed to the d→d* transition of Ni^{II} [$^3A_{2g}\rightarrow{}^3T_{1g}$ (^3F); Table 2]. The surface photovoltage spectra of complexes **1**–**3** match their absorption spectra.

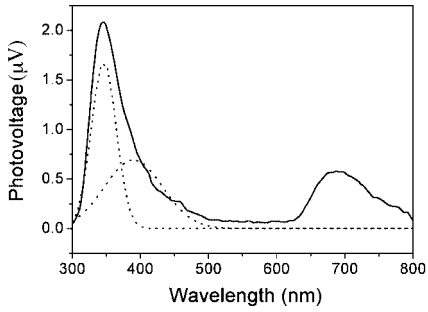

Figure 11. The surface photovoltage spectrum of complex **1**. The dotted lines are the peaks obtained after treatment with Origin 7.0.

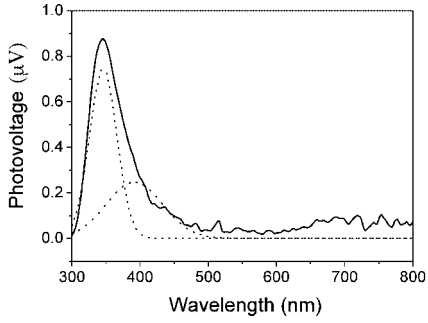

Figure 12. The surface photovoltage spectrum of complex **3**. The dotted lines are the peaks obtained after treatment with Origin 7.0.

Table 2. Assignment of the surface photovoltage spectra.

	λ_{max} [nm]	λ_{max} [nm]	λ_{max} [nm]
1	342	392	690
2	342	387	700
3	342	396	689
Assignment	LMCT	$^3A_{2g}\rightarrow{}^3T_{1g}(^3P)$	$^3A_{2g}\rightarrow{}^3T_{1g}(^3F)$

Comparing the SPV responses of complexes **1**–**3** (Figure 13), it can be seen that without the external electric field the values of the three complexes' response bands are the same, although their intensities are obviously different; complex **1** is the strongest and complex **3** is the weakest. This intensity difference is mainly due to the differences in their structures. Complex **1** is an infinite 3D coordination polymer where the coordination environment of Ni1 is a perfect octahedron. The 2D layer which is formed by two perpendicularly 1D infinite chains is beneficial to the conduction of electrons or holes. Furthermore, another Ni 1D chain which is perpendicular to this 2D layer also provides a transmission passage for the electrons or holes, which means that more electrons diffuse to the surface, resulting in an increase of the SPV response intensities. Complex **2** possesses a infinite 3D structure and the coordination environment of Ni^{II} ion is a perfect octahedron. The planarity of the 2D layer in complex **2** is very good therefore this 2D planar structure is also beneficial to transfer the electrons or holes. Another 1D infinite chain plumbing to the 2D layer intermingles Na^I ions, which may also have certain effects on the transfer of electrons and holes. The intensity of the SPV in complex **2** is lower than that in complex **1**. In complex **3**, the irregularly spaced structure affects the transport of electrons or holes therefore the SPV response's intensity is the weakest. In addition, the types of bonds in the crystal have different effects when it comes to transferring electrons or holes. Complexes **1**–**3** all possess infinite 3D structures. Among them, the 3D structures of complexes **1** and **2** are formed by coordination bonds, whereas in complex **3** the 2D structure is formed by coordination bonds and the 2D layer is further connected into a 3D structure by hydrogen bonds. As hydrogen bonds are weak, their ability to transfer electrons or holes is much lower than that of coordination bonds, therefore the intensity of the SPV of complex **3** is lower than that of complexes **1** and **2**. Moreover, in the range 600–800 nm, it can be seen that the SPV response band of complexes **1** and **2** is a sine wave, whereas the response band of complex **3** shows obvious splitting. These phenomena are mainly attributed to the different symmetries of the Ni^{II} coordination environments: the coordination environment of Ni^{II} in complexes **1** and **2** is a perfect octahedron, whereas in complex **3** it is a distorted octahedron.

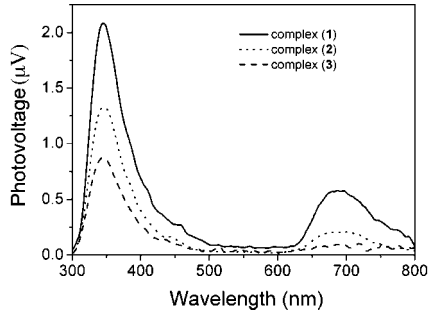

Figure 13. A comparative SPS diagram of complexes **1**–**3**.

FISPS of Complexes

FISPS can determine the direction of the built-in field and the mobile direction of photogeneration carriers. If we apply a positive electric field (the illuminated surface is positive) vertically to the p-type semiconductor surface, whose direction is the same as the direction of the built-in field, the separation efficiency of the photogeneration carriers is increased and the intensity of SPV response increases in the original direction. If a negative electric field, whose direction is opposite to that of the built-in field, is applied, the separation efficiency of the photogenerated carriers reduces and the intensity of the SPV response is weakened, even in the reverse direction. In contrast to p-type semiconductors, the SPV response intensity of n-type semiconductors increases as a negative field is applied and reduces as a positive electric field is applied. The FISP spectrum of complex **1** is given in Figure 14; those of complexes **2** and **3** are analogous with complex **1**. The responses in the range 300–500 nm in all three complexes increase linearly with a posi-

tive electric field, which shows that the direction of this external electric field is consistent with the built-in field. This enhances the separation efficiency of the photoexcited electron–hole pairs and results in an increase of the surface potential, thus confirming that complexes **1**–**3** have p-type semiconductor characteristics.

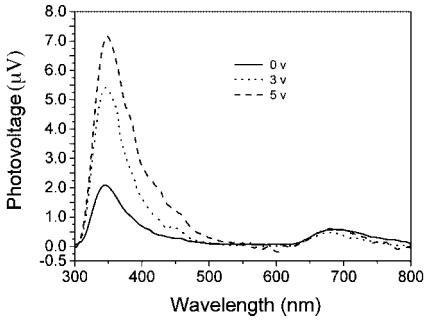

Figure 14. The FISP spectrum of complex **1**. The intensities of the SPV response increase linearly with the external positive electric field.

Conclusion

Three Ni^{II} coordination polymers have been synthesized by hydrothermal methods. Complexes **1** and **2** are both infinite 3D coordination polymers and complex **3** possesses a 2D infinite structure. The surface photovoltage spectra of complexes **1**–**3** show that they all have three positive responses in the range 300–800 nm and all take on p-type semiconductor characteristics. However, the intensities of the SPV response bands are obviously different, mainly due to their different structures. The coordination environment of the Ni^{II} ion affects the shape of the SPV responses, and the FISP spectra confirm the p-type semiconductor characteristics of complexes **1**–**3**.

Experimental Section

Materials and Methods: All reagents were of A.R. grade. IR spectra were recorded in the range 220–4000 cm^{-1} with a JASCO FT-IR/480 spectrophotometer with KBr pellets. The elemental composition of the complexes was determined with a PE-240C analyzer and a TLASMA-II ICP instrument. SPS and FISPS measurements were conducted with the sample in a sandwich cell (ITO/sample/ITO) with the light source-monochromator-lock-in detection technique. All the measurements were performed under atmospheric pressure and at ambient temperature.

$[Ni_2(HCOO)_4(H_2O)_4]_n$ (1): A solution of $NiSO_4{\cdot}6H_2O$ (0.26 g, 1 mmol) in water (10 mL) was added to a solution of *o*-phthalic acid (0.17 g, 1 mmol) in water (10 mL), and 2,2′-bipyridyl (0.08 g, 0.5 mmol) and 5 mL of dmf were added to the above solution. The solution was then transferred into a Parr Teflon®-lined stainless steel vessel, which was sealed and heated to 100 °C for 5 d. After cooling to room temperature, the solution was filtered. Green crystals of complex **1** were obtained by leaving the solution to evaporate at room temperature for about one month. $C_4H_{12}Ni_2O_{12}$ (369.56): calcd. C 13.00, H 3.27, Ni 31.77; found C 13.25, H 3.31, Ni 31.53. IR (KBr): $\tilde{\nu}$ = 3360 cm^{-1}, 3277, 3206 (ν_{OH}); 1574 (ν_{asCOO}); 1378 (ν_{sCOO}); 889, 850, 771 (δ_{C-H}); 566, 357, 311 (ν_{Ni-O}).

$[Na_2Ni(btec)(H_2O)_8]_n$ (2): A solution of $NiSO_4{\cdot}6H_2O$ (0.26 g, 1 mmol) in water (10 mL) was added to a solution of H_4btec (0.13 g, 0.5 mmol) and NaOH (0.08 g, 2 mmol) in water (10 mL), and NaSCN (0.08 g, 1 mmol) and 5 mL of dmf were added to the above solution. The mixture was then transferred into a Parr Teflon®-lined stainless steel vessel, which was sealed and heated to 100 °C for 5 d. After cooling to room temperature, green crystals of complex **2** were collected. $C_{10}H_{18}Na_2NiO_{16}$ (498.93): calcd. C 24.07, H 3.64, Na 9.22, Ni 11.77; found C 24.23, H 3.73, Na 9.03, Ni 11.59. IR (KBr): $\tilde{\nu}$ = 3595 cm^{-1}, 3415 (ν_{OH}); 3029 (ν_{ArC-H}); 1592 (ν_{asCOO}); 1392 (ν_{sCOO}); 1633, 1500, 1439 ($\nu_{ArC\cdots C}$); 1332 (δ_{O-H}); 1145, 974, 912 ($\nu_{C-C,C-O}$); 854, 811, 765, 705 (δ_{C-H}); 537 (ν_{Na-O}), 475 (ν_{Ni-O}).

Table 3. Crystallographic data for complexes **1**–**3**.

	1	**2**	**3**
Empirical formula	$C_4H_{12}Ni_2O_{12}$	$C_{10}H_{18}Na_2NiO_{16}$	$C_7H_9NNiO_7$
Formula weight	369.56	498.93	277.86
Temperature	293(2)	293(2)	293(2)
Wavelength [Å]	0.71073	0.71073	0.71073
Crystal system	monoclinic	monoclinic	orthorhombic
Space group	$P2_1/c$	$C2/m$	$P2_12_12_1$
Unit cell dimensions			
a [Å]	8.600(5)	15.698(10)	7.300(3)
b [Å]	7.068(6)	9.488(7)	9.289(4)
c [Å]	9.219(6)	6.086(3)	14.075(6)
α [°]	90	90	90
β [°]	97.44(3)	93.21(3)	90
γ [°]	90	90	90
Volume [$Å^3$]	555.6(7)	905.1(10)	954.4(7)
Z	2	2	4
D_c [$g\,cm^{-3}$]	2.209	1.831	1.934
F(000)	376	512	568
Goodness-of-fit on F^2	1.105	1.066	1.044
Final R indices [$I > 2\sigma(I)$]	R_1 = 0.0323, wR_2 = 0.0941	R_1 = 0.0291, wR_2 = 0.0816	R_1 = 0.0195, wR_2 = 0.0505
R indices (all data)	R_1 = 0.0349, wR_2 = 0.0957	R_1 = 0.0298, wR_2 = 0.0822	R_1 = 0.0202, wR_2 = 0.0507
Data/restraints/parameters	1270/0/85	1093/2/81	2317/0/169
Absolute structure parameter	–	–	0.013(11)

$[\{Ni(pdc)(H_2O)_2\}\cdot H_2O]_n$ (3): A solution of $NiSO_4\cdot 6H_2O$ (0.26 g, 1 mmol) in water (10 mL) was added to a solution of H_2pdc (0.16 g, 1 mmol) and NaOH (0.08 g, 2 mmol) in water (10 mL). The mixture was then transferred into a Parr Teflon®-lined stainless steel vessel, which was sealed and heated to 160 °C for 5 d. After cooling to room temperature, green crystals of complex **3** were collected. $C_7H_9NNiO_7$ (277.86): calcd. C 30.26, H 3.26, N 5.04, Ni 21.13; found C 30.53, H 3.40, N 5.25, Ni 20.95. IR (KBr): $\tilde{\nu}$ = 3587 cm^{-1}, 3447, 3264, 3187 (ν_{OH}); 3071 (ν_{ArC-H}); 1581, 1549 (ν_{asCOO}); 1394, 1363 (ν_{sCOO}); 1661, 1602, 1479 ($\nu_{ArC\cdots C}$); 1289 (ν_{C-N}); 1182, 1145, 1039 ($\nu_{C-C,C-O}$); 829, 772, 695 (δ_{C-H}); 544, 527 (ν_{Ni-N}); 446, 368, 314 (ν_{Ni-O}).

X-ray Crystallographic Study: Crystallographic data for complexes **1** and **2** were collected on a Rigaku R-AXIS-RAPID diffractometer using graphite-monochromated Mo-K_α radiation (λ = 0.71073 Å) at 293 K. Crystal data for complex **3** was collected on a Smart APEX II CCD diffractometer using graphite-monochromated Mo-K_α radiation (λ = 0.71073 Å) at 293 K. Further details are given in Table 3. All data were corrected for Lorentz polarization factors and empirical absorption. The structures were solved by direct methods and refined by full-matrix least-squares calculations on F^2 using the SHELXTL 97 program. All non-hydrogen atoms were refined anisotropically. Hydrogen atoms were found by mixed methods. Selected bond lengths and angles for complexes **1**–**3** are listed in Table 1.

CCDC-615921 (for **1**), -615922 (for **2**) and -615923 (for **3**) contain the supplementary crystallographic data for this paper. These data can be obtained free of charge from The Cambridge Crystallographic Data Centre via www.ccdc.cam.ac.uk/data_request/cif.

Supporting Information (see also the footnote on the first page of this article): In the Supporting Information, there include three correlated structure figures of complexes **1** and **2**, the IR and UV/Vis spectra of complexes **1**–**3**, the SPS spectrum of complex **2** and the FISPS spectra of complexes **2** and **3**.

Acknowledgments

This work was supported by the National Natural Science Foundation of China (nos. 20571037 and 90201018).

[1] B. Moulton, M. J. Zaworotko, *Chem. Rev.* **2001**, *101*, 1629–1658.
[2] A. Katz, M. E. Davis, *Nature* **2000**, *403*, 286–289.
[3] M. Tominaga, S. Tashiro, M. Aoyagi, *Chem. Commun.* **2002**, 2038–2039.
[4] W. Y. Sun, T. Kusukawa, M. Fujita, *J. Am. Chem. Soc.* **2002**, *124*, 11570–11571.
[5] E. Y. Choi, Y. U. Kwon, *Inorg. Chem. Commun.* **2004**, *7*, 942–945.
[6] S. R. Batten, R. Robson, *Angew. Chem. Int. Ed.* **1998**, *37*, 1460–1494.
[7] R. Sekiya, S. Nishikiori, *Chem. Eur. J.* **2002**, *8*, 4803–4810.
[8] Y. Q. Guo, D. R. Xiao, E. B. Wang, Y. Lu, J. Lü, X. X. Xu, L. Xu, *J. Solid State Chem.* **2005**, *178*, 776–781.
[9] P. J. Hagrman, D. Hagrman, J. Zubieta, *Angew. Chem. Int. Ed.* **1999**, *38*, 2638–2684.
[10] G. B. Deacon, R. J. Phillips, *Coord. Chem. Rev.* **1980**, *33*, 227–250.
[11] M. Melnik, *Coord. Chem. Rev.* **1981**, *36*, 1–44.
[12] M. Kato, Y. Nuto, *Coord. Chem. Rev.* **1988**, *92*, 45–83.
[13] R. H. Wang, F. L. Jiang, L. Han, Y. Q. Gong, Y. F. Zhou, M. C. Hong, *J. Mol. Struct.* **2004**, *699*, 79–84.
[14] D. J. Wang, J. Zhang, T. S. Shi, B. H. Wang, X. Z. Cao, T. J. Li, *J. Photochem. Photobiol. A* **1996**, *93*, 21–25.
[15] Q. L. Zhang, D. J. Wang, J. J. Xu, J. Cao, J. Z. Sun, M. Wang, *Mater. Chem. Phys.* **2003**, *82*, 525–528.
[16] U. Weiler, T. Mayer, W. Jaegermann, C. Kelting, D. Schlettwein, S. Makarov, D. Wöhrle, *J. Phys. Chem. B* **2004**, *108*, 19398–19403.
[17] T. Uekermann, D. Schlettwein, N. I. Jaeger, *J. Phys. Chem. B* **2001**, *105*, 9524–9532.
[18] L. P. Sun, S. Y. Niu, J. Jin, G. D. Yang, L. Ye, *Inorg. Chem. Commun.* **2006**, *9*, 679–682.
[19] T. F. Xie, D. J. Wang, L. J. Zhu, C. Wang, T. J. Li, *J. Phys. Chem. B* **2000**, *104*, 8177–8181.
[20] A. Kokler, J. Gruner, R. H. Friend, K. Mullen, V. Scherf, *Chem. Phys. Lett.* **1995**, *243*, 456–461.
[21] J. S. Kim, B. Lagel, E. Moons, N. Johansson, I. D. Baikie, W. R. Salaneck, R. H. Friend, F. Cacialli, *Synth. Met.* **2000**, *311*, 111–112.
[22] J. Zhang, D. J. Wang, T. S. Shi, B. H. Wang, J. Z. Sun, T. J. Li, *Thin Solid Films* **1996**, *284/285*, 596–599.
[23] H. F. Mao, H. J. Tian, Q. F. Hou, H. J. Xu, *Thin Solid Films* **1997**, *300*, 208–212.
[24] X. Y. Wang, L. Gan, S. W. Zhang, S. Gao, *Inorg. Chem.* **2004**, *43*, 4615–4625.
[25] D. W. Min, S. S. Yoon, C. Y. Lee, W. S. Han, S. W. Lee, *Bull. Korean Chem. Soc.* **2001**, *22*, 1041–1044.
[26] Y. A. Cao, Q. J. Meng, W. S. Yang, J. H. Yao, Y. C. Shu, W. Wang, G. H. Chen, *Colloids Surf., A* **2005**, *262*, 181–186.

Received: August 2, 2006
Published Online: October 31, 2006

